Nanoscale

Nanostructured electrically conductive hydrogels via ultrafast laser processing and self-assembly

Journal:	*Nanoscale*
Manuscript ID	NR-ART-02-2019-001230.R1
Article Type:	Paper
Date Submitted by the Author:	29-Mar-2019

Complete List of Authors:	Tao, Yufeng; Wuhan National Laboratory of Optoelectronics Wei, Chengyiran; Wuhan National Laboratory of Optoelectronics Liu, Jingwei; Wuhan National Laboratory of Optoelectronics Deng, Chunsan; Wuhan National Laboratory of Optoelectronics Cai, Song; Wuhan National Laboratory of Optoelectronics Xiong, Wei; University of Nebraska-Lincoln, Department of Electrical and Computer Engineering; Wuhan National Laboratory of Optoelectronics,

ARTICLE pdf format

Nanostructured electrically conductive hydrogels via ultrafast laser processing and self-assembly

Received 00th January 20xx,
Accepted 00th January 20xx

DOI: 10.1039/x0xx00000x

Yufeng Tao*, Chengyiran Wei, Jingwei Liu, Chunsan Deng, Song Cai and Wei Xiong*

Electrically conductive polymers have emerged as functional materials for future electronics due to their high electrical conductivity, real-time responsiveness, easy film-formation ability and desirable stretchability. However, the previously-developed conductive polymer electronics were still limited in macroscopic hydrogels or films without complicated designs of fine features. Herein, carbon nanotube-doped hydrophilic photoresist was ultrafast laser processed as an absorbent 3D scaffold to fabricate nanostructured electrically conductive hydrogels (NECHs) for the first time. Taking advantage of intermolecular forces, we in-situ interpenetrated π-conjugated poly (3,4-ethylenedioxythiophene) into NECHs by self-assembly to combine fine feature (resolution down to 500 nm, at least two-order accuracy improvement than standard 3D-printing electronics), high electrical conductivity (0.1 - 42.5 Sm^{-1}), device-level mechanical properties and desirable tolerance to humid/acid environments. Consequently, several reliable, nanostructured, metal-free electrical circuits, alcohol micro-sensor, interdigital capacitor, and loop inductors were experimentally identified and characterized. NECHs successfully breaks current limitations by making better use of two photon hydrogelation and highly-conductive polymer. Optical clarity, conductivity, and extensibility of NECHs promises micro energy storage devices, epidermal electronics, nanorobotics and electrical circuit boards for challenging conditions.

Introduction

Multi-functional electronics fabricated via electrically conductive polymer/carbon composite materials are re-establishing the current technological world due to materials' excellent electrical, thermal, optical, mechanical and chemical properties. [1-3] Especially, single-wall and multi-wall carbon nanotubes (SWNT and MWNT) consisted of stable crystal lattice structured on sp^2-bonded carbon atoms of high electrical conductivity (0.17-2 × 10^7 Sm^{-1}), have unique mechanical properties (high stiffness and Young's modulus),[4] ease to be covalently functionalized, and lower toxicity than heavy metal materials.[5] Therefore, SWNT/MWNT attracted considerable attentions as nanofiller to polymeric matrix for functionalization in epidermal/wearable electronics,[6] thermal/optical actuators, bio robotics, disease diagnosis, nature-mimic devices,[7] wound healing, [8] cardiac tissue regeneration,[9] strain sensors and even micro/nano energy devices.[10-12]

On other side, the cationic polythiopene derivative, poly (3,4-ethylenedioxythiophene), known as PEDOT of high energy level (about 5.2 eV),[13,14] sustaining film formation ability, water solubility after blending with poly sodium styrene sulfonate (PSS),[15] chemical stability,[2,16] and higher electrical conductivity outperforming poly aniline/pyrrole and inorganic Si/GaAs semiconductors, which was applicable in organic solar cells, micro super-capacitors, thermoelectric devices, touch planes, display, and stretchable electronics. [11, 17-19]

Polymer/carbon composite materials denoted a disruptive technology in early stage but presented challenges. Recently, several research teams devoted great effort for rationally designed electronic applications, unfortunately, few methods succeeded in 3D dimension formation at nano-scale. As we know, the porous nanocomposite conductive hydrogels (poly aniline and pyrrole) via sol-gel formulations or biological tissues achieved relatively-low conductivity (< 1 Sm^{-1}, Table 1 of supplementary materials).[7,20] Vacuum filtration of CNT-solution, providing only plane-like conductive film without specific designs, required tedious exfoliation/transferring operation.[18] Single photon polymerization of polymer/CNT solution hardly reached sub-micron level resolution.[9] The predominant three dimensional micro-structuring tool, two-photon polymerization (TPP),[21,44] could solidified CNT-doped commercial resin to obtain stiff nanoeletronics,[22] but thiols (such as pentaerythritol tetrakis and ethyl mercaptan) or silane coupling agents used to functionalize CNT were biologically poisonous.[23,24] The widely-used SU-8, Ormocer, or IP-series of photoresists only produced stationary structures in absence of electrical functionality.

It is of huge potentially rewarding to develop NECH-based multi-functional devices to satisfy the impending demand from MEMS, semiconductor industries, biomaterial sciences, or nano engineering. Herein, we modified polymer/MWNT to combine two-photon hydrogelation (TPH) with in-situ self-assembly of PEDOT at microscopic level (Figures 1a and S1).[25,27] TPH was a revolved TPP (Figure S2, supplementary materials) to process

Wuhan National Laboratory of OptoElectronics, Huazhong University of Science and Technology, 1037 Luoyu Road, Wuhan, 430074, China.
Email: wsnwp520@sina.com, weixiong@hust.edu.cn;
Electronic Supplementary Information (ESI) available: [Supplementary information is available by contacting corresponding author]. See DOI: 10.1039/x0xx00000x

composite MWNT-doped, photon-curable materials, generating various NECHs with chemical functional groups as prescribed by digital model with lateral feature sizes down to 200 nm, beyond optics diffraction limit. [25,28] Carbon nanomaterials were expected to advance the properties of extreme 3D objects exceeding the traditional materials science had done at the chemical level. The new composite photoresist contained acrylamide (AC), MWNTs covalently-functionalized via PEG (Figure S5), and hydrophilic diacrylate for electrically conductive micro/nano structures by radical cross-linking reaction.

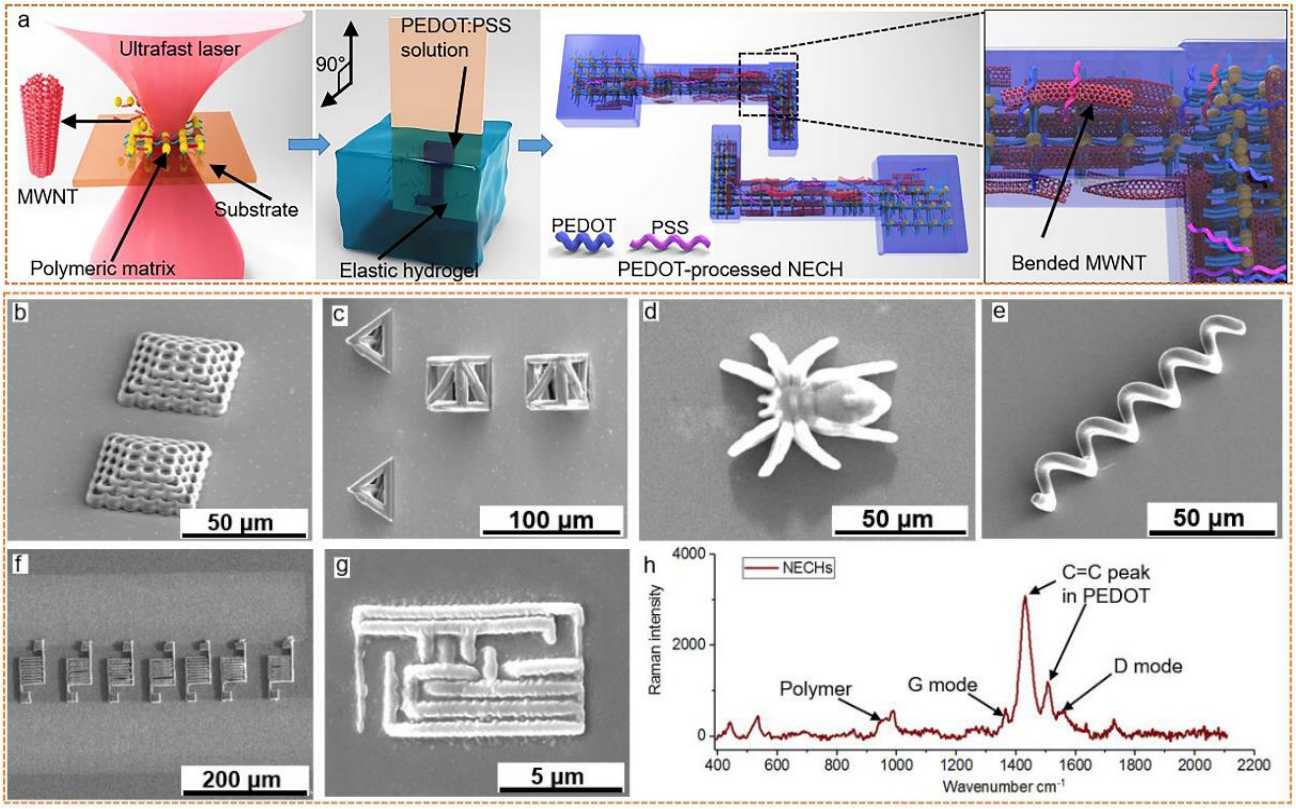

Figure 1. (a) The stepwise nanofabrication contains: 1.two photon hydrogelation (TPH), where voxel was governed by laser intensity and scanning speed, 2.Self-assembly of PEDOT:PSS due to noncovalent π-π interaction and hydrogen bonding. (b) Photonic crystal, (c) Tetrahedrons and cubes (dimension of 45 × 45 × 45 μm^3), (d) 3D spider, (e) Spiral-like inductor, (f) On-chip micro interdigital capacitors, (g) Nano electrical circuit fabricated via the nanofabrication method. (h) Raman spectra of NECHs demonstrating the characteristic peak of PEDOT and MWNTs.

To benefit from self-assembly process, PEDOT:PSS (blended by electrovalent bonds, Figure S6) in solution self-assembled into the unfolded polymeric matrix of NECHs with water diffusion process. PEDOT interacted with MWNT by noncovalent π-π effect: 1.Coating MWNTs to facilitate electron movement.[34-37] 2.Twining round the isolated MWNTs for continuous electron charge transport. 3. MWNT interconnected the folded PEDOT chains as a carbon bridge (Figure S7). Interaction locked PEDOT into the cross-linked for a conductivity-tunable network.[11,27-29,32,33] Hygroscopic PSS formed hydrogen bonding with -COOH/-OH groups of PEG for interpenetration. During self-assembly (NECHs immersed in PEDOT:PSS solution), we confirmed over 215.0% expansion in length without breaking, and excellent resilience (recovered to 95.0 %, Video movie, supplementary material).

Results

Proper design of material ratios provided more than one functionality. Here, hydrophilic diacrylate cleaved by radicals zand cross-linked with other monomeric material to form highly-disorder chain folded polymeric matrix (Equations 1-5, supplementary material), gradient stress of optical tweezer effect and van der Waals force manipulated MWNTs to bend, aggregate and align in the liquid-to-solid phase transform as in-built conductive network.[19] Elastic polymeric matrix offered additional adhesive force due to materials' viscoelasticity, tightly attached to substrate, then was dehydrated, vertically immersed in PEDOT:PSS solution for self-assembly of PEDOT:PSS (Figure 1a).[26] No topological constraints existed (Figures 1b-1h) in the freeform 3D geometry design. The promising feature size could be furtherly modulated by employing suitable laser intensities and exposure time to better than 300 nm.

One-dimensional carbon nanomaterial, MWNT, brought forth multi-fold merits to NECHs: 1. Alignment due to quantum confinement effect inside polymer matrix provided an oriented direction for electron transport.[22,23] 2. Enhancement of mechanical properties to self-support multi-layer, complicated geometries. 3. High surface area (28 m^2/g) of MWNTs increased

interfacial area to hold long-chain PEDOTs as nano sorbents. 4. Improving conductivity of PEDOT as carbon dopant. [30,31]

A fraction of anionics, sodium dodecyl benzene sulfonate (SDBS, 2 wt%, $C_{18}H_{30}NaO_3S$) was mixed into PEDOT:PSS water solution, which possessed acidic anions as dopant to enhance conductivity of PEDOT, improved dispersion of PEDOT in solution as surfactant and softened the long chains of PSSs for easy interpenetration into 3D polymeric matrix.[2,30,34]

Alcohol sensor on-chip and electrical circuits

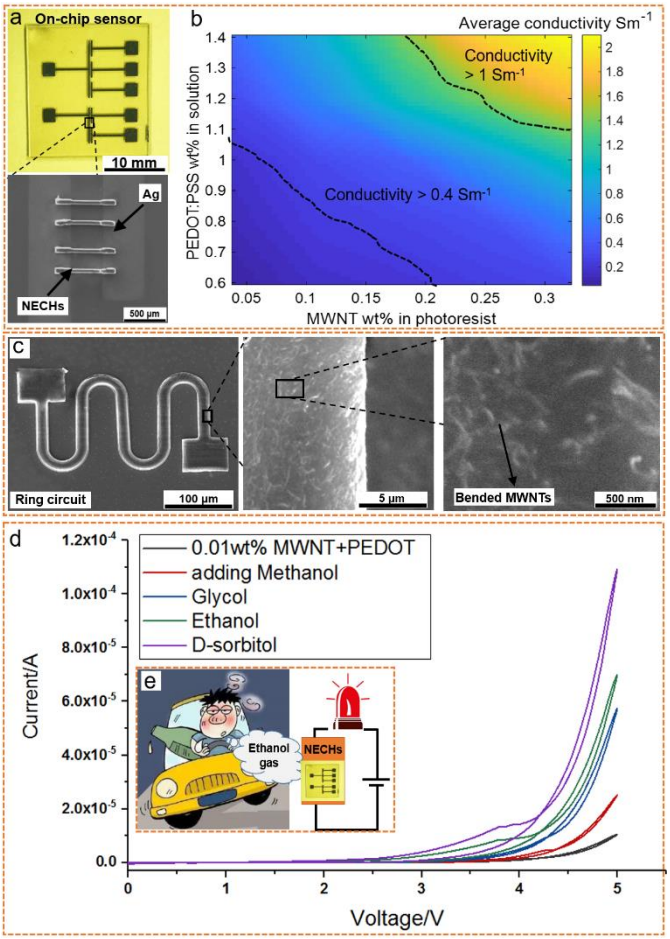

Figure 2. (a) On-chip micron-wire NECHs connecting electrodes (each dimension of 300×40×3 μm³) and zoomed-in SEM images. (b) Conductivity of NECHs related to concentrations of MWNT and PEDOT. (c) Ring circuit fabricated by TPH and its zoomed-in view.(d) A batch of I/V curves of micron wires of NECHs after been humidified by alcohols. (e) Schematic of alcohol-sensor to examine out the drunk car-driver.

We fabricated straightforward micro wire (Figure 2a) and ring circuit (Figure 2c) on chip to investigate the electrical conductivity (Figure 2b). π-conjugate long chain of PEDOT linked junctional points of MWNTs for a more percolation charge transport path. At the given MWNT length in fixed hydrogel, PEDOT:PSS assembled into the embedded MWNTs as percolation network with fewer junctions, decreasing the total junction resistance. Large concentration (0.3 wt%) of MWNTs constituted more percolation pathways at constant volume for higher conductivity.[32,33] Moreover, percolation network varied in stretched or bended volume, unfolded or folded to change conductivity. Significantly different to pure metal or carbon electronics, conductivity of MWNT/PEDOT network reversibly changed by various of alcohol materials including ethanol (C_2H_6O), glycol ($(CH_2OH)_2$), methanol (CH_4O) or D-sorbitol ($C_6H_{14}O_6$), which worked as removable or volatile dopants to transform molecular structures of PEDOT:PSS.[26] This was a new frontier in technology with innumerable and unimaginable sensing potentials. Specially, alcohol-sensitive NECHs easily examined out the drunk car-drivers by testing their exhaled air to prevent the potential traffic accidents (Figure 2e), which would improve safety of all mankind.

To quantitatively measure impedance of NECHs, 30 nm thickness nickel (as sacrifice layer) and 50 nm thickness silver were thermally deposited through mask (FS-300-S6, Fangsheng Optoelectronics) on substrate as electrodes for NECHs. Semi-conductive device analyzer outputted alternating voltages (20 Hz, -5 to 5 V) to electrodes trough tungsten probes (tip diameter was 45 μm) and monitored the transient current-versus-voltage relationship. Lowest impedance (< 15 kΩ by dropping alcohol) exponentially increased to approximately 575 kΩ or higher after dehydration. I/V curves of 20 cycles switched at threshold of 3.1V, little current (< 1.5 μA) below 3.1V, but increased rapidly at high slope of approximate up to 60 μA/V (Figure 2d).

The repeatable sensing ability of NECHs originates from reversible phase separation of the blending material system and the elastic MWNT/polymer/PEDOT matrix. Alcohols contained –COOH and –OH functional groups to attract the hydrophilic PSS, the formed hydrogen bonding competed with the ionic bonding between PEDOT and PSS, and pulled PSS out as phase separation, therefore, PEDOT molecules aggregated to increase electrical conductivity.

MWNT-embedded network improved conductivity of the original insulting hydrogel (0.007 Sm^{-1} at 0.05 wt%, 0.12 Sm^{-1} at 0.2 wt%, 0.8 Sm^{-1} at 0.3 wt% respectively). Self-assembly of PEDOTs got another one-magnitude conductivity improvement, which became wide-band tunable by alcohols from 0.1 to 42.5 Sm^{-1}(conductivity was calculated via equation 6 when volume expansion was neglected). Pure deionized water could improve the conductivity slightly, and 10 wt% ethanol in deionized water solution only magnified about average 5 times of conductivity, 30 wt% magnified average 11 times, 50 wt % magnified average 32 times, 99%+ purity ethanol magnified average 92 times. The electric performance of NECHs was summarized in Figure S4. Fortunately, paralleling arrangement of NECHs between electrodes would furtherly decline resistance without bottom limitation of resistance.

Micro interdigital capacitor

Energy storage devices hold key to solve the growing issue of finite nature sources of fossil fuels around the earth.[35-37] Specially, micro interdigital capacitor (MIC), equalled paralleling electrodes for higher storage ability, could harvest energy from nano-generators, MEMS and micro robotics, or supply power to wearable or epidermal electronics. [36,37] Here, We demonstrated a variety of ultra-thin MICs based on PEDOT-processed NECHs

(Figure 3) such as common capacitor (Figure 3a), MIC (Figures 3b, S8 and S9), and on-chip array of MICs (Figure 3c). Thickness of in-plane MICs was down to minimum 2 μm (single layer), as demonstrated by 3D micrograph (Figures S8 and S10).

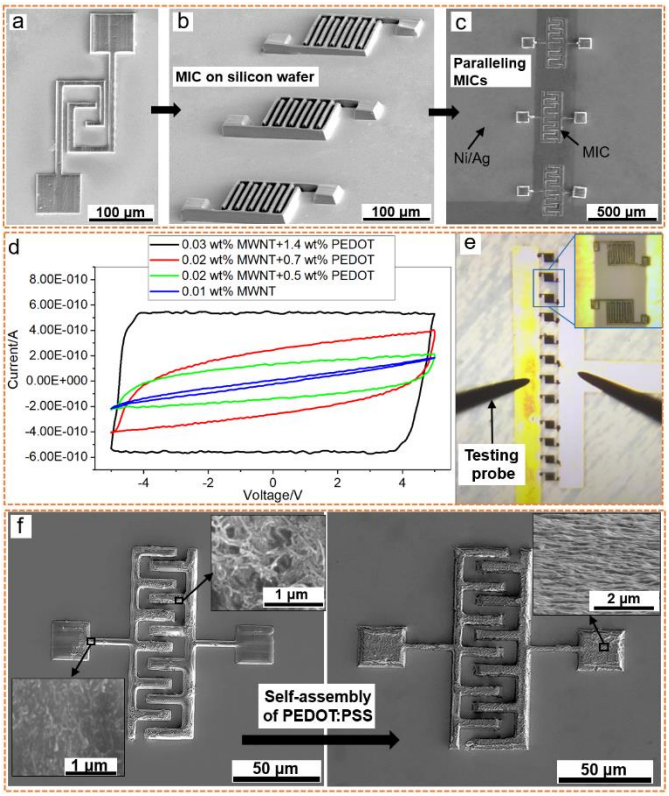

Figure 3. (a) A common capacitor consisted of single pair of electrodes. (b) MIC of five pairs of electrodes. (c) Paralleling MICs (of six pairs of electrodes) connecting electrodes on silicon. (d) Hysteresis loop-like I/V currents, which gradually opened by increasing concentrations of MWNT and PEDOT. (e) The integrated MICs by TPH bridging two metal electrodes. (f) SEM images of MIC before and after immersion in PEDOT solution.

Current-to-voltage (I/V) relationship of alternative voltage-applied MICs presented different electric hysteresis loops in absence of pseudo capacitive materials sandwiching the MWNT/PEDOT electrodes (Figure 3d), higher concentration of MWNTs and PEDOTs open the loops as symbol of higher capacitance. For NECHs on the order of Figures 3a→3b→3c, the average capacitance increased: 0.56pF→1.7pF →3.4pF tested by semi-conductive device analyzer, physical volume increased: 1.8e5 μm^3→3.3e5 μm^3→9.1e5 μm^3, and capacitance density changes: 0.311e-2 $fF/\mu m^3$→0.52e-2$fF/\mu m^3$→0.37e-2$fF/\mu m^3$. A relatively low capacitance of bare Ag electrode was 211 fF.

Freedom model design allowed integration of numerous MICs in single chip (Figure 3e) to increase capacitance, which maybe substantially developed to nanostructured super-capacitors by integration and adjustment of MWNT/PEDOT:PSS concentrations. MICs were also potential for further uptake of electrolyte ions from aqueous agents in a short diffusion pathway. [25,30] Surface morphology of MICs was reconfigured by uptake of SDBS-doped PEDOT:PSS (Figures 3f, S9 and S10), from MWNT-aggregated rough surface→ swelled surface → twinkled surface covered by PEDOT:PSS .

Spiral-like inductors and 3D structures

TPH on composite MWNT/polymer photoresist and post-processing by self-assembly of PEODT altered how prototype, develop and regulate spatial and temporal distribution of electronics in three-dimension. Thank to this remarkable advantage, we successfully fabricated 3D electrically conductive nanostructures of small-scale from different computer models in Figures 1 and 4. The hollowed structures without fillers stood on substrate independently (Figures 1, 4a-4c), the surrounding white points scattered on structures were nanoclusters of MWNTs.

The spiral-like NECHs, serving as electrical micro inductors (diameter was about 5 μm), suspend in air at height over 12 μm (Figure 4c). No breaking or collapsing happened after self-assembly of PEDOT due to MWNT reinforcement (Young's modulus increased from 300 Mpa to 900Mpa, Figure 4e, theoretical Young's modulus of MWNT could exceed 500 GPa, stiffness exceeds 80 Gpa). [39,42] Aggregated MWNTs constrained volume variation or deformation, declined the water-induced volume expansion from over 200 % to only about 115 % (Figure 4f). Maximum breaking length perpendicular to laser scanning direction was over 200% (tested on a milli-meter level hydrogel fabricated using same parameters) if MWNTs concentration < 0.05 wt%, deceased to about 160% at 0.1 wt%, further decreased to 130% at 0.15 wt% MWNTs, and became brittle and easy to beak if this concentration was over 0.32 wt%.

We performed Raman spectroscopy to confirm the selective distribution of PEDOT in self-assembly around the on-chip NECHs. Initial dimension of MWNTs (diameter of 10-15 nm, length of 0.3-5 μm) was condensed during polymerization process and the intersection with PEDOT: PSS, causing a slight blue shift of tangential mode (G-band) peak shifting to 1381 cm^{-1} and disorder mode (D-band) peak shifting to 1545 cm^{-1}. Radial breathing mode (wavenumber less than 300 cm^{-1}) of MWNTs became subtle and was overwhelmed by characteristic peaks of polymer. Strong 1441 cm^{-1} peak originated from symmetrical stretching vibration of C=C bonding of PEDOT, 1507 cm^{-1} denoted its antisymmetric stretching vibration (Figure 1h). Raman mapping image centering on peak of C=C chain of PEDOT was scanned through a square area of 50 × 50 μm^2 at each pixel, which reflected the shape of 'TPH' word pattern, showing PEDOT molecules preferentially assembled into NECHs, not the substrate. (Figure 4d).

Expansion or shrinkage of NECHs also replied on polymer materials and the smoothly-scanning line-to-line strategy. Different to pure acrylate-based polymers, the Young's modulus of the self-assembled hydrogel via mechanics testing system show a wide variable range from 150 Mpa to 900 Mpa due to different material ratio and solvent retention, making the fabricated NECHs both soft and stiff for various multi-layer

structures. Both compressive and tensile properties were affected by MWNTs concentration.

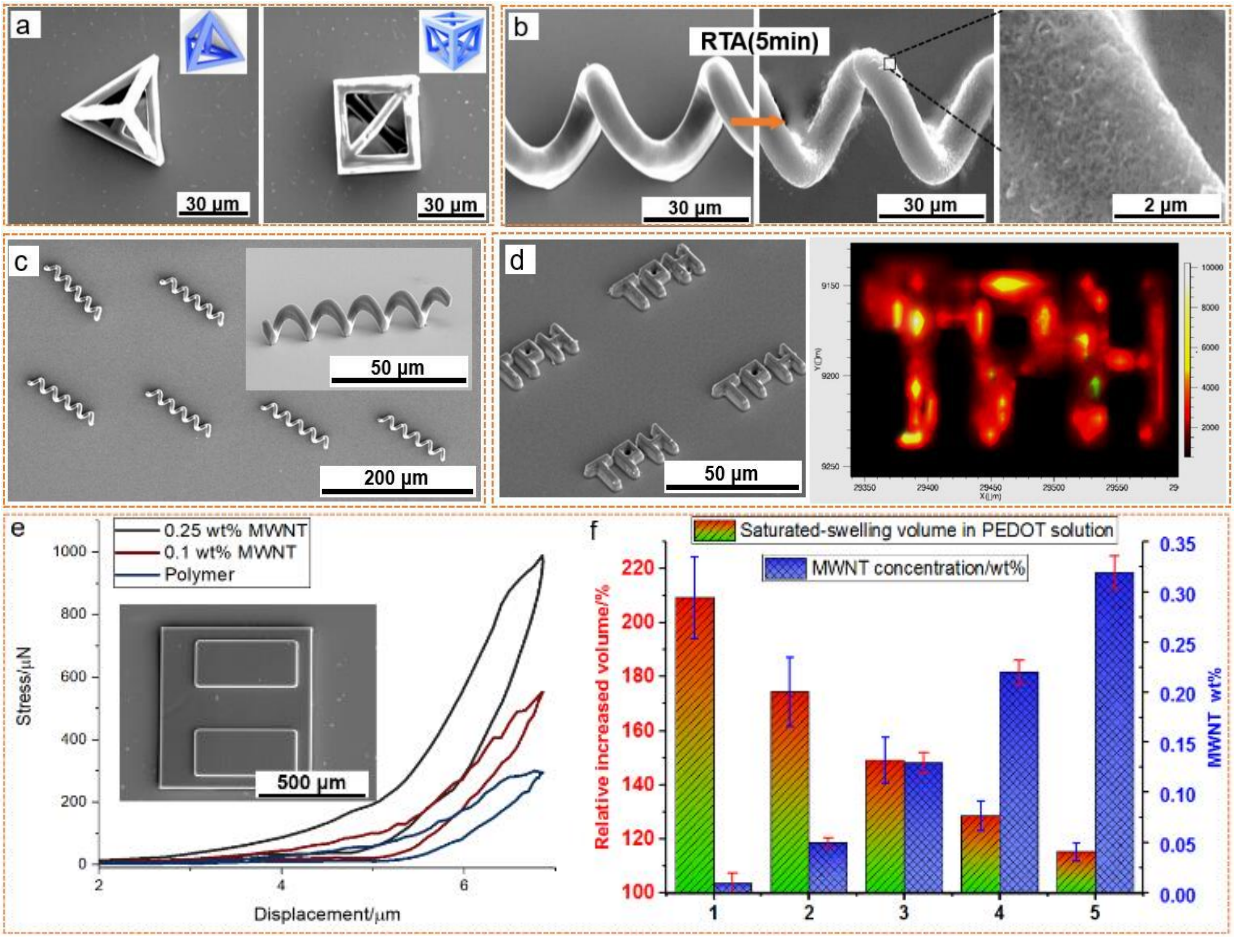

Figure 4. Digital models and NECHs fabricated via TPH. (a) The hollowed tetrahedrons and cubes. (b) SEM images of hydrogels after being selectively RTA (400 °C, 5 min). (c) Spiral-like inductors on silicon wafer, no sacrifice layer or additional support. (d) 'TPH' word hydrogel and Raman mapping image. (e) The fabricated bulk hydrogel for compressive and tensile test to figure out Young's modulus of NECHs affected by MWNTs. (f) Swelling ratios of NECHs in PEDOT:PSS solution determined by MWNT concentration.

Soft polymer materials for ultrafast laser process requires much lower optical power for cross-linking than metal materials and forms less heating crack in and after formation.[23,37,38,41] No additional reducing agents or heavy metals (Cu, Ag or Au) were deposited,[42]thus reducing environmental pollution. Importantly, oxidation reaction or acid corrosion usually devastated the structural integrity and conductivity of electronics became negligible to hygroscopic NECHs. Elasticity and high surface-volume ratio of NECHs provided additional adhesive force for interconnecting with the sweating human skins. [43] We suggest against the long-time RTA/sintering on NECHs, although high temperature (>400 °C) initiated the transition of PEDOT from a Fermi glass to a semi-metal through molecular organization[2, 34] for high conductivity and thermally evaporate the polymeric matrix, but semi-crystaline PEDOT bulks would lose the host of benefits of hydrogels and broke continuous electron transport, eventually leading to conductivity declining.

In our work, NECHs fabricated by the TPH and self-assembly of PEDOT:PSS are metal/ion-free, conductivity-tunable, highly-stretchable with high tolerance to the sweating human skin, humidity or weak acid environment, much smaller size than the reported hydrogels. Moreover, the existing macroscopic bio applications (gelation sponge or biological swellable scaffold) would become more injectable, wearable and implantable, and applicable in diagnosis electronics for tissue, eardrum and cytosol via TPH on PEG-DA/MWNT. [6,8,9] The PEDOT-processed NECHs could play multi-fold important roles of providing electric stimulation to small biological tissues as extracellular media, or sensing the weak electrocardiography and electromyography signals from human or animals.

Experiment

Ultra-fine 3D formation quality of NECHs and morphology of carbon nanomaterials were characterized by environmental scanning electron microscope (ESEM). Raman spectroscopy reflected out the photon-initiated chemistry process and distribution of PEDOT. We determined electrical performance of NECHs using an advanced semiconductor parameter analyzer. Mechanical properties of NECHs were tested by nanoidentation

technique. Hygroscopic swelling phenomenon of MWNT-embedded hydrogel featured with mass uptake and the residual stress variation inside of NECHs, which may lead to small local deformation (Video movie). Thermo gravimetric analysis and precision electrical scale (Explorer, OHAUS, resolution of 10 μg) both shown the NECHs gain approximate 3.1% weight by uptake of PEDOT: PSS in swelling process.

PEG grating method functionalizing MWNTs

We chemically processed the carboxyl-functionalized MWNTs to covalently grate PEG groups to MWNTs through acyl chlorination reaction. Thionyl chloride ($SOCl_2$, Mw=118.97), or known as sulfurous oxychloride, was used to replace hydroxyl of carboxylic groups by chlorine group firstly, then MWNT-$COCl_2$ reacted with amino polyethylene glycol (PEG-NH_2, C_2H_7NO, Mw =61.0528) to form covalent amido bonding with PEG groups (Figure S5f). We added 50 mg MWNT-COOH to mixture of butylene oxide (10 wt%) and thionyl chloride (90 wt%) at 60 °C for over two days, and microporous filtered out sediment (pore diameter equals 1200 nm). The sediment was washed by benzene-toluene, and vacuum dried as intermediate products (MWNT-$COCl_2$), then was mixed with 40 mL PEG-NH_2 under N_2 gas protection at 80 °C over four days to get PEG functionalized MWNTs, the final products was vacuum dried for photoresist preparation. Best solubility of PEG-MWNTs in our experiment reached 3.7 mg/mL in ethanol at a much smaller water-contact angle than thiol-MWNTs (Figure S5d).

Photoresist preparation

All reagents, used for photoresist, development and self-assembly, were at high purity 99.9+%, and commercially available (purchased from Sigma-Aldrich). Mw denoted the mol weight of materials. We prepared AC ($C_7H_{10}N_2O_2$, 0.7 mg, Mw=71.08), PEG-DA ((C_3H_3O).(C_2H_4O)n.(C_3H_3O), 4 ml, Mw=575), methylene blue (MC, 0.03mg, Mw = 319.86), ethanol (0.2 mL), PEG-MWNTs (3 mg, obtained by PEG-grating reaction), and di-trimethylolpropane tetraacrylate (Di-TMPTTA, $C_{24}H_{34}O_9$, 1mL, Mw=466), and mixed them. Subsequently, the mixture underwent 5 min ultrasonic agitation (power: 60 W, frequency: 30KHz, SB-800DTD, SCIENTZ) in dark, followed by magnetic stirring for 4 hours at room temperature and purified at low-speed centrifugation (6000 rpm, 20 min) to remove MWNT aggregations.

Two photon hydrogelation

An oil-immersed objective lens (60 ×, N.A. = 1.4) focused laser beam to the liquid-to-substrate interface. Because we implanted a 2D, high-speed, galvanometric scanning mirror to move laser focus, the entire optical system was fixed on an air-floating platform to isolate vibrational interference, NECHs maintained an ultrafine spatial resolution (< 300 nm) with suitable optical parameters of ultrafast laser pulse. [44,45]

Morphology characterization

Before characterization through Environmental Scanning Electron Microscope (ESEM) at acceleration voltages of 5 kV (QUANTA 200, FEI) for secondary-electron and backscattered-electron images, we freezing-dried NECHs in absence of metal sputtering for details of structure. Energy Dispersive X-Ray Spectroscopy (Edx) was in-situ collected to determine elements of NECHs (Figure S11). Moreover, to quantify specific dimension, we utilized an advanced 3D super-depth microscopes, VK-X1000 of KENYENCE to scan NECHs at subwavelength accuracy.

Semi-conductive parameters test

Electrical performance of NECHs required cutting-edge measuring technology, here, we used a semi-conductive devices analyser including a high-resolution digital source meter (B1500A, Keysight) and operational platform (MPS150, Cascade Microtech) to determine the I/V characters of NECHs. Double tungsten probes touched the NECHs or electrodes when applied the altered voltage and collect transient current (pA resolution).

Thermo gravimetric analysis

Uptake of PEDOT:PSS and water retention were vital parameters for NECHs, and were evaluated by the advanced thermogravimetric analysis (TGA) technique. We placed samples in a thermally-controlled chamber and monitored by thermogravimetric analyser (Pyris-1, Perkinelmer). Ambient temperature of NECHs was up to 70 °C and weight resolution was small down to 0.1 μg. Temperature ramped up at 5 °C/min from 30 °C to 60 °C to dehydrate hydrogel and record weight loss.

Raman microspectroscopy

To elucidate the underneath photochemical mechanism, Raman microspectroscopy were performed through a Raman spectrometer at laser wavelength of 532 nm (InVia, Renishaw) ranging from 200 to 2000 nm using 60 × objective lens (N.A. = 0.75). Laser power irradiating on NECHs was 5 mW. Data interrogation of Raman spectra was at time interval of 3 sec each. Mapping covered NECHs at each pixel and using 1440 cm^{-1} peak. Raman spectrum was analysed using WiRE software.

Micro mechanical properties measurements

Mechanical properties of NECHs were investigated by a micromechanical testing instrument (FT-MTA02, FemtoTools). A micron-robotic system combines the FT-FS1000 mechanical force sensor (containing an ultrafine probe, tip radius is only 2 μm) with the FT-UMS1002 (optical microscope system with 7 time magnification) for tensile, compressive and adhesive forces tests.

Conclusions

We prepared a new hydrophilic photoresist incorporating MWNTs (concentration was up to 0.32 wt%) for two photon hydrogelation, and utilized the fabricated MWNT-doped hydrogels for self-assembly of conductive polymer in solution. PEG-MWNTs sustained desirable dispersion quality, bio-compatability and solubility in composite photoresist. Multi-functional NECHs were experimentally identified (electrical circuits, sensors, capacitors and inductor). Experiment shown the MWNT-embedded polymeric matrix sustains sufficient free space to interpenetrate with PEDOTs to enhance mechanical properties and electrical conductivity (from about 0.1 Sm^{-1} to over 42.5 Sm^{-1} by alcohol materials), which surpassed the macroscopic conductive hydrogel at least two-order magnitude.

Interestingly, NECHs were hybrids, combining the properties of polymers (low-temperature processing, transparency and resilience) with those of carbon materials (hardness, chemical stability, and electrical conductivity) after self-assembly, and still kept the pre-designed 3D nanostructures and ultrafine feature. We clearly observed the embedded MWNTs, and multi-layer 3D formation. Using the proposed method, tremendous multi-functional chip-scale devices far beyond the demonstrations could be fabricated, and the conventional soft electronics were expected to scale down to mesoscopic level.

Conflicts of interest

There are no conflicts to declare.

Acknowledgements

This research was financially supported by the National Key R&D Program of China (2017YFB1104300), the National Natural Science Foundation of China (61774067), the National Science Foundation (CMMI 1265122), and the Fundamental Research Funds for the Central Universities (HUST:2018KFYXKJC027), National Science Youth Fund of china (61805094,51705141), China Postdoctoral Science Foundation (2017M622417).

All author thank to the facility support of the center for Nanoscale characterization & devices (CNCD), WNLO of HUST.

Notes and references

1 L. Pan, A. Chortos, G. Yu, Y. Wang, S. Isaacson, R. Allen, Y. Shi, R. Dauskardt, Z. Bao, An ultra-sensitive resistive pressure sensor based on hollow-sphere microstructure induced elasticity in conducting polymer film. *Nat. Commun.* 2014, **5**, 3002.

2 Y.Wang, Chenxin Zhu, R. Pfattner, H.P. Yan, L.H. Jin, S.C. Chen,F. Molina-Lopez, F. Lisse, J. Liu, N. Rabiah, Z. Chen, J. W. Chung, C. Linder, M.F. Toney, B. Murmann, Z.N Bao, A highly stretchable, transparent,and conductive polymer. *Sci.Adv.* 2017, **3**, e1602076

3 N. Hu, Y. Karube, C. Yan, Z. Masuda, H. Fukunaga, Tunneling effect in a polymer/carbon nanotube nanocomposite strain sensor. *Acta. Mater.* 2008, **56**(13), 2929-2936

4 C.Y. Wang, K.L. Xia, H.M. Wang, X.P. Liang, Z. Yin, Y.Y. Zhang, Advanced Carbon for Flexible and Wearable Electronics, *Adv. Mat.* 2018, 1801072

5 S. Gong, W. Cheng, One‐Dimensional Nanomaterials for Soft Electronics, *Adv. Electron. Mater.* 2017, **3**, 1600314.

6 H. W. Yuk, B.Yang, Lu, X. H.Zhao, Hydrogel bioelectronics, *Chem. Soc. Rev.* 2018, 10.1039/C8CS00595H

7 H.L. Sun, H. A. Klok, Z. Y. Zhong, Polymers from Nature and for Nature，*Biomacromolecules*. 2018, **19**, 1697−1700

8 X. Zhao, B.L. Guo, H. Wu, Y.P. Liang, P.X. Ma, Injectable antibacterial conductive nanocomposite hryogels with rapid shape recovery for noncompressible hemorrhage and wound healing, *Nat. Comm.* 2018,**9**, 2784

9 Y. B. Wu, L. Wang, B.L. Guo, P.X. Ma, Interwoven Aligned Conductive Nanofiber Yarn/Hydrogel Composite Scaffolds for Engineered 3D Cardiac Anisotropy, *ACS Nano*. 2017, **11**, 5646−5659

10 T. Q. Trung, N. E. Lee, Flexible and Stretchable Physical Sensor Integrated Platforms for Wearable Human‐Activity Monitoringand Personal Healthcare, *Adv. Mater.* 2016, **28**, 4338.

11 H. Wang, C. Wang, M. Jian, Q. Wang, K. Xia, Z. Yin, M. Zhang, X. Liang, Y. Zhang, Superelastic wire-shaped supercapacitor sustaining 850% tensile strain based on carbon nanotube@graphene fiber, *Nano Res.* 2018, **11**, 2347.

12 N.H. Liu, Y.H Gao, Recent progress in micro-supercapacitors with in-plane interdigital electrode architecture, *Small* , 2017, 1701989

13 B. Y. Lu, H.W. Yuk, S.T. Lin, N.N Jian, K. Qu, J.K. Xu, X.H. Zhao, Pure PEDOT:PSS hydrogels, *Nat. Comm.*2019,**10**, 1043

14 E. Roh, B.U. Hwang, D. Kim, B. Y. Kim, N.E. Lee, Stretchable, Transparent, Ultrasensitive, and Patchable Strain Sensor for Human-Machine Interfaces Comprising a Nanohybrid of Carbon Nanotubes and Conductive Elastomers, *Acs Nano,* 2015, **9**(6), 6252-6261

15 D. Yoo, J. Kim, J.H. Kim, Direct synthesis of highly conductive poly(3,4-ethylenedioxythiophene):poly(4-styrenesulfonate) (PEDOT:PSS)/graphene composites and their applications in energy harvesting systems, *Nano. Res.* 2014,**7**(5), 717-730

16 D. Huang, T. Goh, J. Kong, Y.F. Zheng, S.L. Zhao, Z. Xu, A.D. Talyor, Perovskite solar cells with a DMSO-treated PEDOT: PSS hole transport layer exhibit higher photovoltaic performance and enhanced durability. *Nanoscale.* 2017, **9**(12), 4236-4243

17 Y.X. Zeng, X.Y. Zhang, Y. Meng, M.H. Yu, J.N. Yi, J.N. Yi, Y.Q.Wu, X.H. Lu, Y.X. Tong, Achieving Ultrahigh Energy Density and Long Durability in a Flexible Rechargeable Quasi-Solid-State Zn-MnO2 Battery, *Adv. Mat.* 2017, **29**(26),1700274

18 Z. S. Wu, K. Parvez, X.L. Feng, K. Mullen, Graphene-based in-plane micro-supercapacitors with high power and energy densities, *Nat. Comm.* 2013, **4**, 2487

19 T. Park, C. Park, B. Kim, H. Shin, E. Kim, Flexible PEDOT electrodes with large thermoelectric power factors to generate electricity by the touch of fingertips, *Energ. Environ. Sci.* 2013, **6**(3), 788-792

20 Y.Shi, C. Ma, L. Peng, G. Yu, Conductive “Smart” Hybrid Hydrogels with PNIPAM and Nanostructured Conductive Polymers. *Adv.Funct.Mater.* 2015, **25**(8),1219-1225

21 X.W. Wang, Y. Gu, Z.P. Xiong, Z. Cui, T. Zhang, Silk-molded flexible, ultrasensitive, and highly stable electronic skin for monitoring human physiological signals. *Adv. Mat.* 2016, **24** (9), 1336-1342

22 W. Xiong, Y.S. Zhou, W.J. Hou, L.J.Jiang, M. Mahjouri-Samani, J. Park, X.N. He, Y.Gao, L.S. Fan, T. Baldacchini, J. Silvain, Y.F. Lu, Laser-based micro/nanofabrication in one, two and three dimensions, *Front. Optoelectron.*2014, DOI 10.1007/s12200-015-0481-3

23 W. Xiong, Laser-Directed Assembly of Aligned Carbon Nanotubes in Three Dimensions for Multifunctional Device Fabrication. *Adv. Mat.* 2016, **28** (10), 2002

24 A. N. M. Nasir, N. Yahaya, N.N.M.Zain, V. Lim, S. Kamaruzaman, B. Saad, N. Nishiyama, N. Yoshida, Y. Hirota, Thiol-functionalized magnetic carbon nanotubes for magnetic micro-solid phase extraction of sulfonamide antibiotics from milks and commercial chicken meat products, *Food. Chem.* 2019, **276**, 458-466

25 A. S. Aricò, P. Bruce, B. Scrosati, J. M. Tarascon, W. Schalkwijk, Nanostructured materials for advanced energy conversion and storage devices, *Nat. Mat.* 2005,**4**, 366-377

26 H.Q.Zhou, Y. Zhang, C.K. Mai, S.D. Collins, T.Q. Nguyen, G.C. Bazan, A.J. Heeger, Conductive Conjugated Polyelectrolyte as Hole-Transporting Layer for Organic Bulk Heterojunction Solar Cells, *Adv. Mat.* 2014, **26**(5), 780-785

27 M. Malinauskas, Ultrafast laser processing of materials: from science to industry. *Light-Sci. Appl.* 2016, **5**, e16133

28 E. Scarpa, E.D. Lemma, R. Fiammengo, M.P. Cipolla, F. Pisanello, F. Rizzi, M. De Vittorio, Microfabrication of pH-responsive 3D hydrogel structures via two-photon

polymerization of high-molecular-weight poly(ethylene glycol) diacrylates. *Sensor. Actuat. B-Chem.* 2019, **279**, 418-426

29 A. Urrios, C. Parra-Cabrera, N. Bhattacharjee, A.M. Gonzalez-Suarez, L.G. Rigat-Brugarolas, 3D-printing of transparent bio-microfluidic devices in PEG-DA. *Lab Chip*, 2016, **16**, 2287–2294

30 K. Wang, L. Tian, T.H. Wang, Z. Q. Zhang, X.J. Gao, L. Wu, B. Fu, X.H. Liu, Electrodeposition of alginate with PEDOT/PSS coated MWCNTs to make an interpenetrating conducting hydrogel for neural interface, *Compos. Interfaces.* 2019, **26**(1), 27–40

31 C.Q. Li, X.J. Cheng, L. M. Wu, Fabrication of conjugated polymer/carbon nano-tube composite materials for capacitors, *Mater. Res. Exp.* 2019, **6**(3), 036302

32 Y.H. Li, B. Zhou, G. Q. Zheng, X.H. Liu, T. X. Li, C. Yan, C. B. Cheng, K. Dai, C. T. Liu, C. Y. Shen, Continuously prepared highly conductive and stretchable SWNT/MWNT synergistically composited electrospun thermoplastic polyurethane yarns for wearable sensing , *J. MATER. CHEM. C.* 2018, **6** (9), 2258-2269

33 J. Rivnay, S. Inal, B.A. Collins, M. Sessolo, E. Stavrinidou, X. Strakosas, C. Tassone, D.M. Delongchamp, G.G. Malliaras, Structural control of mixed ionic and electronic transport in conducting polymers, *Nat. Comm.* 2016, **7**, 11287

34 O. Bubnova, Z.U. Khan, H. Wang, S. Braun, D.R. Evans, M. Fabretto, P. Hojati-Talemi, D. Dagnelund, J.B. Arlin, Y. H. Geerts, Semi-metallic polymers, *Nat. Mater.* 2014, **13**(2),190-194

35 S. Grimme, Do Special Noncovalent π–π Stacking Interactions Really Exist, *Angew.Chem.Ed*.2008,**47**,3430-3434

36 D.P. Malenov, G.V. Janjic, V.B. Medakovic, M.B. Hall, S. D. Zaric, Noncovalent bonding: Stacking interactions of chelate rings of transition metal complexes, *Coordin. Chem. Rev.* 2017, **345**(15),318-341

37 S. Pegel, P. Potschke, G. Petzold, I. Alig, S.M. Dudkin, D. Lellinger, Dispersion, agglomeration, and network formation of multiwalled carbon nanotubes in polycarbonate melts, *Polymer,* 2008, **49**(4), 974-984

38 D. Alemu, H.Y. Wei, K. C. Ho, C.W. Chu, Highly conductive PEDOT:PSS electrode by simple film treatment with methanol for ITO-free polymer solar cells, *Energ. Environ. Sci.* 2012, **5**(11), 9662-9671

39 Q. Jiang, C.S. Wu, Z.J. Wang, A.C. Wang, J. He, Z.L. Wang, H. N. Alshareef, MXene Electrochemical Microsupercapacitor Integrated with Triboelectric Nanogenerator as a Wearable Self-charging Power Unit, *Nano Energy.* 2018.**01**.004, 266-272

40 B. K. Yun, H. S. Kim, Y. J. Ko, G. Murillo, J. H. Jung, Interdigital electrode based triboelectric nanogenerator for effective energy harvesting from water, *Nano Energy*, 2017, **36**, 233-240

41 Z.Y.Liu, Z.S. Wu, S. Yang, R.H. Dong, X. L. Feng, K. Mullen, Ultraflexible In-Plane Micro-Supercapacitors by Direct Printing of Solution-Processable Electrochemically Exfoliated Graphene, *Adv. Mat.* 2016, **28**(11), 2217-2222

42 S.Lee, M. Wajahat, J. H. Kim, J. Pyo, W. S. Chang, S.H. Cho, J. T. Kim, S.K. Seol, Electroless Deposition-Assisted 3D Printing of Micro Circuitries for Structural Electronics, ACS Appl. Mater. Interfaces. 2019, 11, 7123−713

43 S. Yao, P. Swetha, Y. Zhu, Nanomaterial‐Enabled Wearable Sensors for Healthcare, *Adv. Healthcare Mater.* 2018, **7**, 1700889

44 J.F. Xing, M.L. Zheng, X.M. Duan, Two-photon polymerization microfabrication of hydrogels: an advanced 3D printing technology for tissue engineering and drug delivery, *Chem. Soc. Rev.* 2015, **44**(15): 5031-5039

45 S. H. Lee, J.J. Moon, J.L. West, Three-dimensional micropatterning of bioactive hydrogels via two-photon laser scanning photolithography for guided 3D cell migration, *Biomaterials.*2018, 29(20), 2926-296

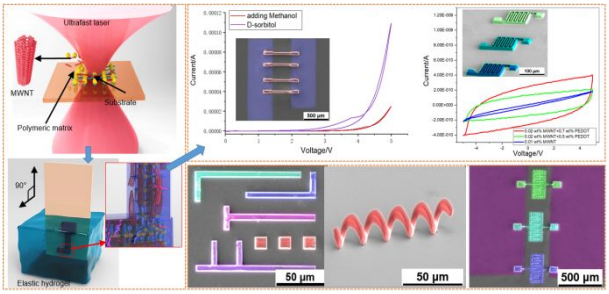

Ultrafast laser processing MWNT/polymer composite materials for absorbent polymeric matrix and self-assembly of PEDOT:PSS to obtain nanostructured electrically conductive hydrogels.